



2D-FEM LIQUEFACTION ANALYSIS FOR RIVER DIKE IN TYPICAL LOWLAND AREA OF JAPAN

Hiroshi ABE¹

SUMMARY

In the 1995 Hyogoken-nambu Earthquake, liquefaction of the ground was observed at Hyogo and Osaka Prefectures in Japan. A study performed to assess the extent of damage to civil engineering structures demonstrated that extensive damage had been caused to the embankments at the river mouth of the Yodogawa River in Osaka City in ground locations subject to liquefaction as well as in quay-walls at the Port Island in Kobe City. Despite the success in developing the liquefaction study method, the recent earthquakes which took place during the 1993 Kuroki Earthquake, the 2000 Tottori-ken-seibu Earthquake, and the 2003 Tokachi-oki Earthquake caused much damage to the ground and dike structures in the disaster areas. The reasons for the delay in the execution of studies may be the lack of development work to establish models for the stress behavior of earth-structures in view of the greater complexity of the stress conditions in earth-structures rather than in level ground. The author is in the process of developing the TOTAL system, an evaluation system designed primarily for the assessment of the seismic resistance of earth-structures. This paper presents the simulation results for the shaking table tests on a ground with embankment and the damaged reclamation land dike, river dike, and road bank in typical lowland area of JAPAN using the two-dimensional FEM direct non-linear liquefaction analysis program EFFCTD. This program is a relatively simple program developed by combining the hysteresis type function model which is an extension of the non-linear elasticity analysis method with dynamic test leading to excess pore water pressure.

The shaking table test results show clear evidence that not improved ground with embankment has a different behavior from level ground. With the EFFCTD program, it was possible to reproduce the measurement vertical displacement results obtained in the shaking table tests and the damaged Yodogawa River dikes.

INTRODUCTION

The author is in the process of developing the TOTAL system (Abe [1]), an evaluation system designed primarily for the assessment of the anti-liquefaction earth-structures.

¹ Professor, Gunma College of Technology, Gunma, JAPAN. Email: abe@cvl.gunma-ct.ac.jp

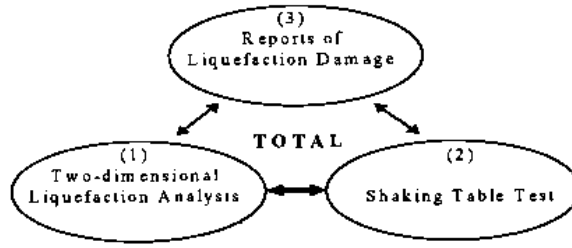


Figure 1 TOTAL system

The general outline of the TOTAL is shown in **Figure 1**. In the first stage, (1) establishment of a Liquefaction analysis program cord based on effective stress method, (2) carrying out of 1G model shaking table tests and/or centrifuge dynamic model tests, and (3) collecting and systematically ordering of information from studies of ground with embankment. In the second stage, the work involved a comparison of the analytical results of (1) the two-dimensional liquefaction analysis and the experiment results of (2) shaking table tests so as to ascertain the performance capability and the suitability range of the analysis program. In the third stage, the task was to create a system capable of reproducing the case of damage under (3) reports of liquefaction from the analyzing program under (1). After this, the analysis was performed with the data for the existing earth-structures and foundation grounds under the control of the Metropolis of Tokyo to establish a system for predicting liquefaction damage and for examining appropriate preventive measures.

This paper describes the simulation results for the shaking table tests on a ground with embankment using program EFFCTD obtained in the second stage of the system construction work. This paper also presents the simulation results for the damaged earth-structure in Japan using the EFFCTD.

The EFFCTD permits seismic response analysis using direct integration time history and is based on the effective stress method using two-dimensional FEM. The merit of the EFFCTD program lies in its usefulness in modeling earth-structures subjected to liquefaction under plane strain conditions. The demerit of the EFFCTD program is that it cannot handle structures in three-dimensional conditions. Nor can it simulate the dynamic behavior of input motions with two horizontal directions. The EFFCTD code uses the non-linear elasticity theory for a one-phase system, It is relatively simple direct non-linear method developed by combining of the hysteresis type function model (the modified Ramberg-Osgood model) which is an extension of the non-linear elasticity analysis for the one-phase system with the laboratory dynamic element test systems leading to excess pore water pressure.

Hysteresis type function model

The equation of modified R-O's skeleton curve (Tatsuoka [2]) can be expressed by the following Eq. (1).

$$\gamma = \frac{\tau}{G_{\max}} \left(1 + \alpha |\tau|^\beta \right) \quad (1)$$

Where τ, γ , and G_{\max} are the shear stress, shear strain, and shear modulus at $\tau = 0.0$, respectively; α and β are non-linear parameters in the modified R-O model.

Tatsuoka also established α and β using the dynamic soil parameters as shown below.

$$\alpha = \left(\frac{2}{\gamma_{0.5} G_{\max}} \right)^{\beta} \quad (2)$$

$$\beta = \frac{2\pi h_{\max}}{2 - \pi h_{\max}} \quad (3)$$

Where $\gamma_{0.5}$ is the shear strain at $G/G_{\max} = 0.5$, and h_{\max} is the maximum damping ratio.

Tatsuoka have considered $\gamma_{0.5}$ for the large strain with liquefaction stage as shown Eq. (4)

$$\gamma_{0.5} = \gamma_r = \frac{\tau_f}{G_{\max}} \quad (4)$$

Where γ_r is the reference shear strain, and τ_f is the shear strength, respectively.

From Eq. (4), Eq. (2) can be expressed as Eq. (5)

$$\alpha = \left(\frac{2}{\tau_f} \right)^{\beta} \quad (5)$$

From Eq. (5) and $G_{\max} \approx G_0 (\gamma = 1.0 \times 10^{-6})$, Eq. (1) can be expressed by Eq. (6)

$$\gamma = \frac{\tau}{G_0} \left(1 + \alpha' \left| \frac{\tau}{\tau_f} \right|^{\beta} \right) \quad (6)$$

with

$$\alpha' = 2^{\beta} \quad (7)$$

Where G_0 is the initial shear modulus.

Equation (3) and Equation (7) are based on the equivalent linear method using the relationship between the scant shear modulus and the damping ratio versus the varied shear strain amplitude. Using h_{\max} , G_0 , and τ_f , the shear strain γ can be determined simply. Originally, the R-O model does not have the concept of shear strength. We introduced the concept of shear strength into the modified R-O model by using Eq. (4) to make the effective stress liquefaction analysis. Differentiating Eq. (6), we can determine the tangent shear modulus G_t for the incremental dynamic response, and substitute this for the plain strain elasticity matrix D. The branch curves of the modified R-O hysteresis loops can be determined by applying Masing's rule. The unloading hysteresis curve is expressed by Eq. (8a), and reloading curve is expressed by Eq. (8b).

$$\gamma - \gamma^* = \frac{1}{G_0} (\tau - \tau^*) \left[1 + \alpha' \left| \frac{\tau - \tau^*}{2\tau_f} \right| \right]^\beta \quad (8a)$$

$$\gamma + \gamma^* = \frac{1}{G_0} (\tau + \tau^*) \left[1 + \alpha' \left| \frac{\tau + \tau^*}{2\tau_f} \right| \right]^\beta \quad (8b)$$

Where τ^* and γ^* are the shear stress and shear strain at the branch points, respectively. The effective stress σ' under the two-dimensional plane strain condition is expressed by Eqs. (9a) and (9b).

$$\{\sigma'\} = \{\sigma\} - \{m\}u \quad (9a)$$

with

$$\{m\} = \{1 \quad 1 \quad 0\}^T \quad (9b)$$

Where σ is total stress, u is the excess pore water pressure, and vector m corresponds to Kronecker's δ indicating the tensor. In order to maintain the constant total stress value against a changing pore water pressure, the excess pore water pressure u_m is expressed by Eq. (10).

$$u_m = \sigma'_{mi} - \sigma'_m \quad (10)$$

Where σ'_{mi} is the initial effective mean normal stress and, σ'_m is the effective mean normal at any time step.

Shear modulus G_0 is expressed by Eq. (11).

$$G_0 = G_{0i} (\sigma'_{mi} - u_m)^{0.5} \quad (11)$$

with

$$\sigma'_{mi} = \frac{1 + 2K_0}{3(1 + K_0)} (\sigma'_{y,static} + \sigma'_{x,static}) \quad (12)$$

Where G_{0i} is the initial shear modulus under a standard initial effective mean normal stress σ'_{mi} , and K_0 is the coefficient of earth pressure at rest, $\sigma'_{x,static}$ and $\sigma'_{y,static}$ are the initial effective normal stress in the $X - Y$ plane (horizontal-vertical) using the self-weight static analysis, respectively.

Kokusho et al. [3] established an effective stress path algorithm by using the empirical formula of excess pore water pressure buildup proposed by Seed et al. and the accumulative damage concept proposed by Annaki and Lee.

The empirical formula by Seed is expressed by Eqs. (13a) and (13b).

$$r_N = \left[\frac{1}{2} (1 - \cos \pi r_u) \right]^\xi \quad (13a)$$

with

$$r_N = N / N_l, \quad r_u = u / \sigma'_{ci} \quad (13b)$$

In which r_N is cyclic number ratio, N_l is the induced liquefaction cyclic number, r_u is the excess pore water pressure ratio, σ'_{ci} is the initial confining stress, and ξ is the Seed's empirical parameter.

Shear strength τ_f is expressed by Eq. (14).

$$\tau_f = C' \cos \phi' + (\sigma'_m - u_m) \sin \phi' \quad (14)$$

Where C' and ϕ' are the cohesion and the internal friction angle in term of effective stress, respectively.

From Eq. (9) through Eq.(14), the effective mean normal stress σ'_m , the shear modulus G_0 , and the shear strength τ_f changed by the excess pore water pressure u_m are obtained at each time step.

Analytical results

An element simulation of liquefaction test

The shaking table tests have demonstrated that there are certain areas beneath the embankment with poor lateral confinement, and to overcome this problem suitable measures have been applied to permit the calculation of the excess pore water pressure even in these areas. The effect of the presence of lateral confinement on the water pressure was investigated by authors using undrained cyclic hollow cylinder torsion test (Abe [1]). Test result is shown in **Figure 2**. It can be seen that if the lateral displacement was confined, the water pressure did reach the overburden stress, whereas without this confinement, the water pressure did not reach this overburden stress. This test result was incorporated into the EFFCTD. We have defined a new value which is the lateral flow factor L . This factor is defined as Eq. (15)

$$L = K / K_0 \quad (15)$$

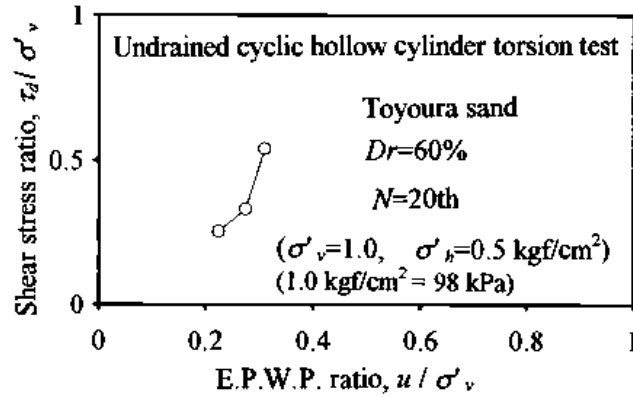


Figure 2 Cyclic hollow cylinder torsion test

Where K is the ratio of the initial effective horizontal stress σ'_{xi} to initial effective vertical stress σ'_{yi} , $L = 1.0$: lateral displacement confinement, $L < 1.0$: lateral displacement un confinement.

We have concluded that elements for which L assumes 1.0 or below 1.0 are finite elements with a weak lateral confining effect. The maximum excess pore water pressure value of the beneath the embankment are controlled by the relation between shear stress ratio and E.P.W.P. ratio under lateral displacement free (see **Fig. 2**).

The EFFCTD was checked against the test results quoted in the shaking table test (Abe [1]). The outcome of these verification procedures suggest that the program is capable of reproducing the measurement values (acceleration amplitude and excess pore water pressure) of shaking table test with practically complete agreement. The verification checks using the shaking table tests and the existing ground with embankment, however, produced results differing from the measurement data for the settlement of the embankment crest. The vertical displacement of the embankment has become very small displacement values in the EFFCTD. The authors have made improvements designed to cause any residual vertical displacement (Abe [4]). From the reports of liquefaction damage, the embankment crest subsides easily in a large earthquake. The 1st factor is the value q of the stress path at a failure line in $q - p'$ stress plane

($p' = \sigma'_m$, $q = \frac{\sigma'_1 - \sigma'_3}{2}$). The 2nd factor is an increment maximum shear stress $\Delta\tau_{\max}$ on the fail-

ure line using the increment value of the dynamic horizontal shear stress $\Delta\tau_{xy,dynamic}$. If the ground lateral displacement keeps being fixed, this increment dynamic horizontal shear stress $\Delta\tau_{\max}$ does not contribute to vertical displacement. When the periphery of the level ground is liquefied, the lateral displacement confining effect decreases. The dynamic maximum shear stress $\Delta\tau_{\max}$ grows on the failure line, the settlement of the embankment has become large. Thus the embankment crest causes vertical displacement under the lateral displacement free. We have defined a new value which is the vertical displacement factor of beneath the embankment (Abe [1]). As a computation algorithm, the stress path q is replaced with an equivalent nodal force and the dynamic maximum shear stress is converted into an equivalent nodal force by using a

settlement conversion factor $F_{settlement}$. Thus the equivalent nodal force f_{equi} is expressed by Eq. (16).

$$f_{equi} = F_{settlement} \times \Delta\tau_{max} \quad (16)$$

Where $\Delta\tau_{max}$ is expressed by σ'_x, σ'_y , and $\Delta\tau_{xy,dynamic}$

The settlement conversion factor $F_{settlement}$ was incorporated into the EFFCTD program. The most suitable settlement conversion factor is 0.5. An advanced EFFCTD program has now been established to make such evaluation possible. (2) Verification results

The author has performed undrained cyclic hollow cylinder torsion test (Toyoura sand, $D_r = 60\%$, $K = \frac{\sigma'_{x,0}}{\sigma'_{y,0}} = 0.5$, $\sigma'_{m0} = 65.66 \text{ kN/m}^2$, 0.1 Hz) for relation between vertical displacement values and lateral displacement confining conditions. The author has performed simulation studies for 24 seconds from the start of cyclic shear loading (1 Hz, 24th). The experiments under lateral displacement fix and the analytical results for the input shear stress amplitude, response shear strain, excess pore water pressure, and shear stress-effective normal stress chart determined from the time histories are shown in **Figure 3**. The experiments under

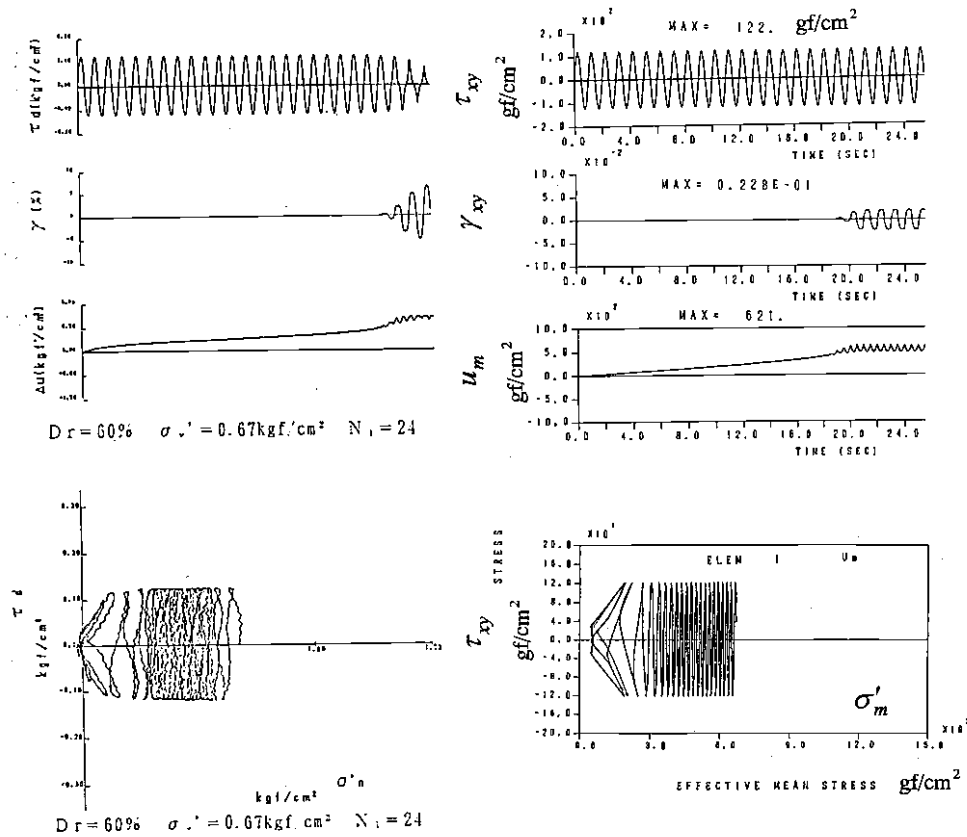


Figure 3 Cyclic hollow cylinder torsion test and EFFCTD analytical result (lateral disp. fix)

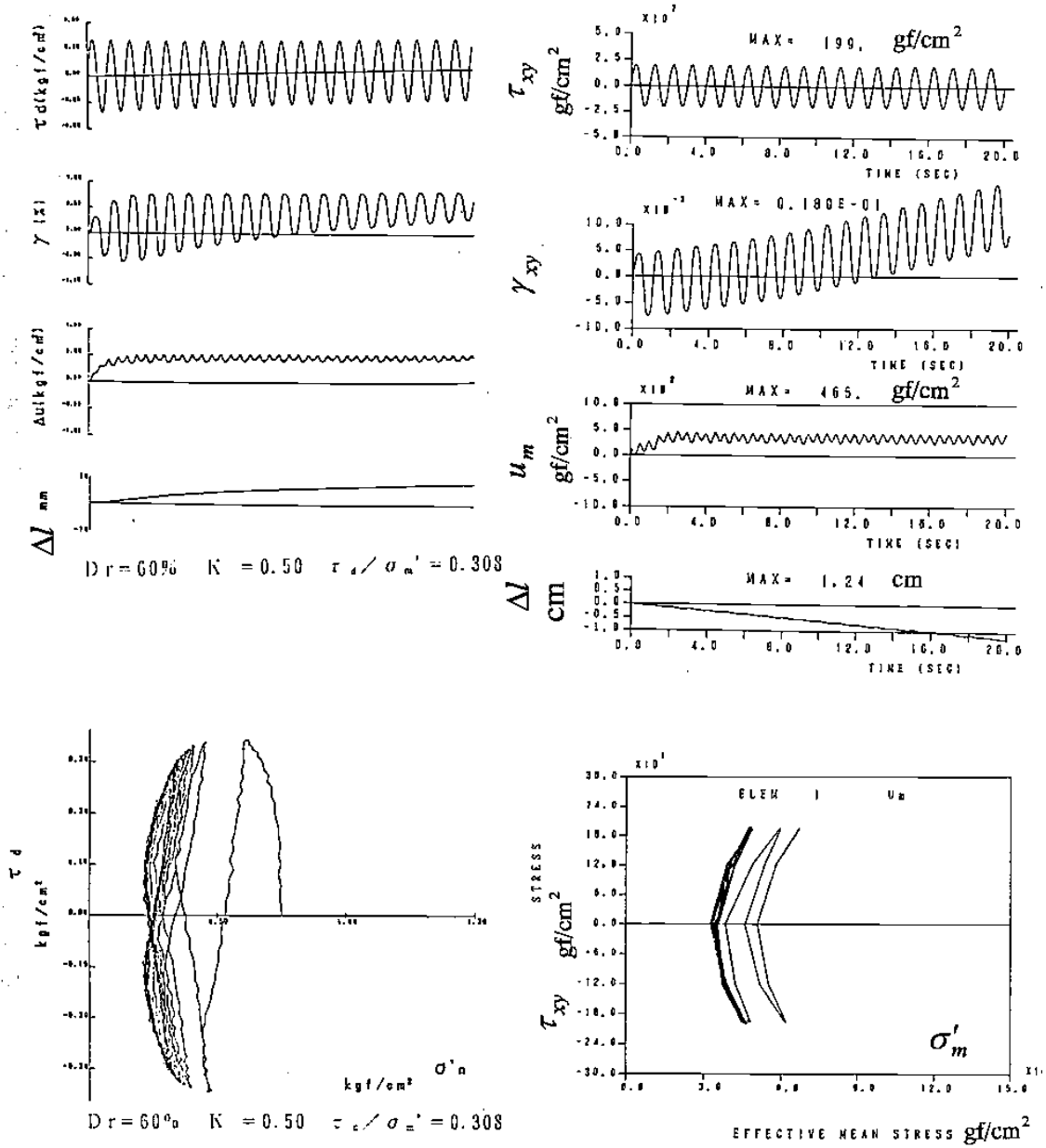


Figure 4 Cyclic hollow cylinder torsion test and EFFCTD analytical result (lateral disp. free)

lateral displacement free and the analytical results are shown in **Figure 4**. From the simulation performed for the lateral displacement fix or free conditions, the experiments and analytical results were in practical agreement.

Analysis for shaking table test

From a total of three types of liquefaction shaking table test and EFFCTD results, the measurement settlements and the analytical results are shown **Table 1**. And, **Figure 5** shows analytical deformation chart for the earth-dam model of Cambridge Univ. The embankment crest settlement values obtained from the EFFCTD led to results that suggest general agreement with

Table 1 Shaking table test results and EFFCTD analytical results

Liquefaction shaking table test	Measurement settlement of embankment crest	Analytical Settlement of embankment crest
Centrifuge shaking table test (Earth-dam, Cambridge Univ., see Fig. 4)	.Experiment No. III 1.924mm (0.18 sec)	After 0.18 sec 1.600mm
1G shaking table test (ground with embankment, unimproved ground, TMG (Abe [1]))	Liquefaction level 12-13mm (15 sec)	After 7.0 sec 7mm
Centrifuge shaking table test (ground with embankment, unimproved ground, TMG)	Liquefaction level 12mm (2.0 sec)	After 2.0 sec 10mm

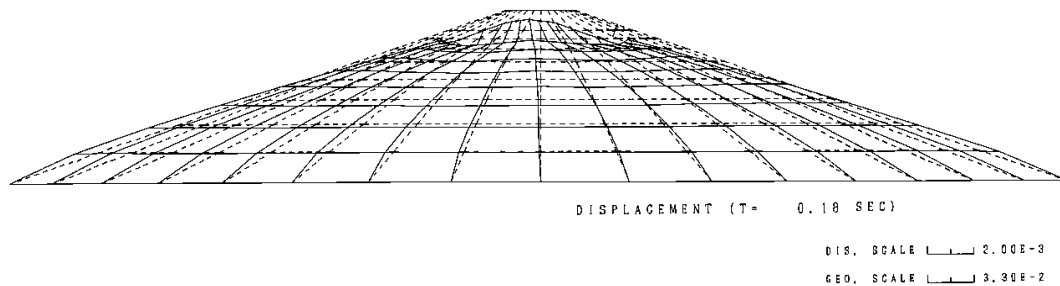


Figure 5 EFFCTD analytical result (Earth-dam, Cambridge Univ.)

the measurement values.

Blind test for shaking table test

Ten types of the blind test simulation were performed using the EFFCTD for a total of nine types of 50G centrifuge dynamic model test (three unimproved ground with embankment models and improved ground with embankment models using six types solidification method). The centrifuge dynamic test was conducted by P.W.R.I (Matsuo et al.[5]). The shaking table test results show clear evidence that not improved ground with embankment has a different behavior from level ground. For the blind test, analytical conditions were given only a ground with embankment size, static and dynamic soil parameters, and a seismic ground motion. Figure 6 shows the relation between analytical results and shaking table test results ($50 \times$ measurement displacement value). The ten post-quake embankment crest settlement values obtained from the EFFCTD led to results that suggest general agreement with the ten measurement values.

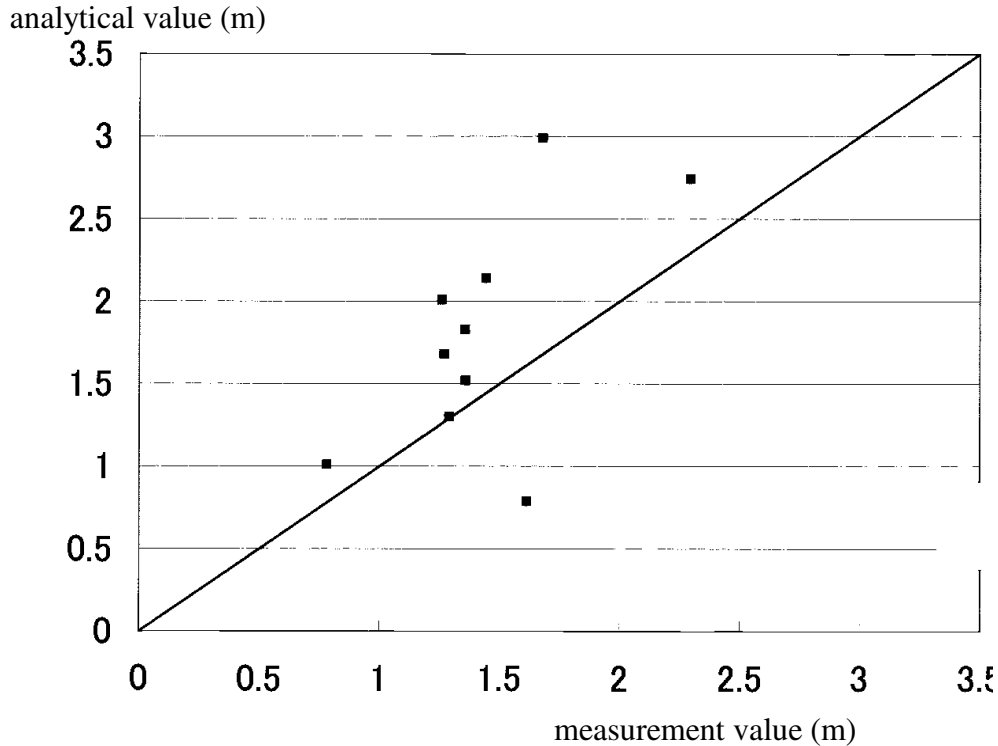


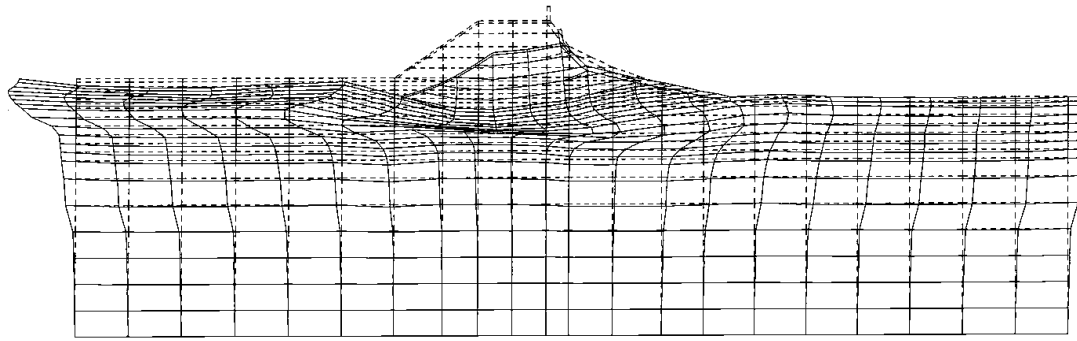
Figure 6 comparison between EFFCTD analytical result and measurement results

Table 2 Measurement results of damage report and EFFCTD analytical results

Liquefaction damage point	Measurement Settlement of embankment crest	Analytical Settlement of Embankment crest
Hachirogata front dike(Nihonkai-cyubu, 1983)	FD6+900 point 1.9m	After 40 sec 1.8m
Yodo-river west bank (Hyogoken-nambu,1995) Denpo watergate, No main bed, see Fig 7	1.5m	After 40 sec 1.4m
Yodo-river west bank (Hyogoken-nambu,1995) Denpo watergate, Dike with main bed, see Fig 8	1.6m	After 40 sec 1.3m
2nd Shinmei road bank (Hyogoken-nambu,1995)	0.2m	After 40 sec 0.35m

Analysis for damaged earth structures

The reports of liquefaction damage existing earth structures (Abe et al. [6]) and the analytical results for the residual settlement are shown **Table 2**. The foundation grounds for the Yodogawa

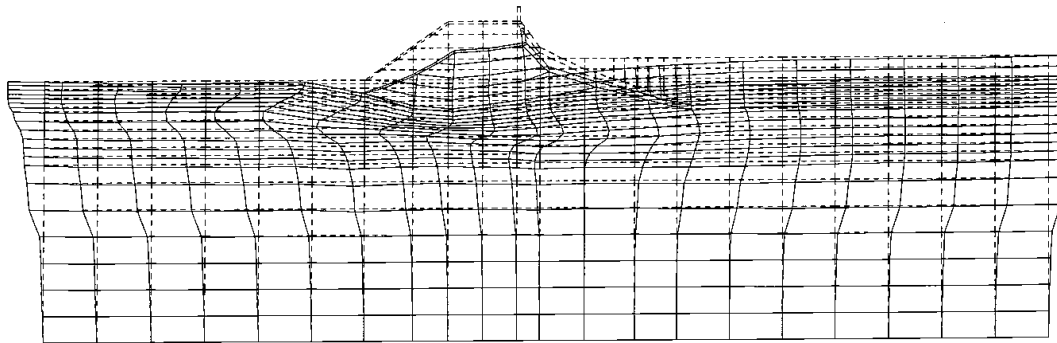


DISPLACEMENT (T= 40.00 SEC)

DIS. SCALE 1 2.00

GEO. SCALE 1 5.02

Figure 7 Analytical deformation chart of Yodogawa River dike not main bed



DISPLACEMENT (T= 40.00 SEC)

DIS. SCALE 1 2.00

GEO. SCALE 1 5.02

Figure 8 Analytical deformation chart of Yodogawa River dike with main bed

River models were composed about 10m in thickness saturated loose alluvial sandy layer located on the about 20m in thickness saturated soft clay. From the damage report, the ground failure was not generated in soft clay layer though the liquefaction was generated in the loose sandy layer.

As two case studies, analytical post-quake deformation chart of the Yodogawa River dike no main bed and the dike with main bed are shown in **Figure 7** and **Figure 8**, respectively. The computation results of the Yodogawa River models are capable of reproducing the vertical deformations of the loose sandy layer. However, the program still failed to produce results in

agreement with the no damage soft clay layer. These results are suggesting that the reformed method is essential to forecast a post-quake clay layer deformation

CONCLUSIONS

The author has developed the TOTAL system for evaluation of the seismic resistance of earth structures taking into account the problems of soil liquefaction and have conducted research on anti-liquefaction measures adapted to the environment of the Tokyo Lowland and the static and dynamic characteristics of the ground. To evaluate the seismic design of earth structure, it will be necessary to make a precise assessment of the post seismic deformation. The simulation study was based on the computer program EFFCTD. This code was seen to be capable of reproducing the dynamic behavior of the ground with embankment model in a satisfactory manner.

REFERENCES

1. Abe H. "Shaking Table Test for Sandy Ground with Embankment." Proc. of JSCE, No.554/III-7, 1996:1-17.
2. Tatsuoka F. "Hysteresis Type Function Model for Dynamic Soil Deformation." New Civil Eng. System, Soil Mechanics (III), 1981:244-252. (in Japanese)
3. Kokusho T., Esashi Y., and Sakurai, A. " Numerical Simulation on Liquefaction." CRIEPI Report, No.381023, 1982.(in Japanese)
4. Abe H. "Aseismic Design of Earth Structure for High Level Seismic Force." JSCE Earthquake Engineering Committee Report, 2000,:118-132. (in Japanese)
5. Matsuo, O., Okamura M., and Tamura S. " Centrifuge Modeling Tests of Ground with Embankment Toe Solidification Method for Anti-liquefaction Effect." Public Works Research Institute Ministry of Construction, PWRI No.3688, 2000. (in Japanese)
6. Abe H., Mori H., Fukutake K., and Fujikawa S. "Investigation and Analytical Evaluation of Damage to Levee Caused by Liquefaction in Hyogoken-Nambu Earthquake." Proc. of JSCE, No.568/III-39, 1997: 89-99. (in Japanese)